ACS APPLIED MATERIALS & INTERFACES

Research Article

www.acsami.org

Effect of PTB7 Properties on the Performance of PTB7:$PC_{71}BM$ Solar Cells

Chap Hang To,[†] Annie Ng,[‡] Qi Dong,[†] Aleksandra B. Djurišić,*[,†] Juan Antonio Zapien,*[,§] Wai Kin Chan,[⊥] and Charles Surya[‡]

[†]Department of Physics, The University of Hong Kong, Pokfulam Road, Hong Kong Island, Hong Kong

[‡]Department of Electronic and Information Engineering, The Hong Kong Polytechnic University, Kowloon, Hong Kong

[§]Center of Super Diamond and Advanced Films (COSDAF) and Department of Physics and Materials Science, City University of Hong Kong, Tat Chee Avenue, Kowloon Tong, Hong Kong

[⊥]Department of Chemistry, The University of Hong Kong, Pokfulam Road, Hong Kong Island, Hong Kong

Supporting Information

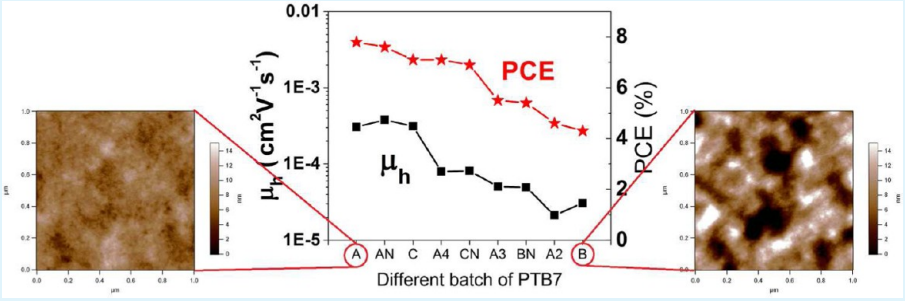

ABSTRACT: The effect of poly[[4,8-bis[(2-ethylhexyl)oxy]benzo[1,2-b:4,5-b′]dithiophene-2,6-diyl][3-fluoro-2-[(2-ethylhexy)-carbonyl]thieno[3,4-*b*]thiophenediyl]] (PTB7) properties on the optical properties, charge transport and photovoltaic performance of PTB7:[6,6]-phenyl C_{71} butyric acid methyl ester ($PC_{71}BM$) blend films is investigated. We found that the variations in the molecular weight (M_w) and polydispersity index (PDI) of PTB7 mainly affect the phase separation and charge transport (hole mobility) in the blend films. The optical properties are also affected, but the increase in the extinction coefficient does not necessarily imply increased power conversion efficiency. The obtained power conversion efficiency for optimized thickness varied from 4.8% to 7.8% depending on the properties of PTB7. The wide range of obtained power conversion efficiencies illustrates the importance of optimizing the M_w and PDI to optimize bulk heterojunction morphology and achieve high performance solar cells.

KEYWORDS: *polymer solar cells, spectroscopic ellipsometry*

1. INTRODUCTION

Poly[[4,8-Bis[(2-ethylhexyl)oxy]benzo[1,2-b:4,5-b′]dithiophene-2,6-diyl][3-fluoro-2-[(2-ethylhexy)carbonyl]thieno[3,4-*b*]-thiophenediyl]] (PTB7) is a low band gap donor polymer of significant interest for applications in bulk heterojunction polymer solar cells.[1−16] High power conversion efficiencies are typically reported for PTB7:[6,6]-phenyl C_{71} butyric acid methyl ester ($PC_{71}BM$) blend films, with a number of reports exceeding 5%,[1,4,5,7,8,10−13,15] although in some cases lower efficiencies ≤4%,[2,5,6] are reported. Among various factors, such as PTB7:$PC_{71}BM$ ratio and solvent used,[13] the photovoltaic performance is also affected by the molecular weight of PTB7.[15] Increased efficiency of cells with higher molecular weight PTB7 was attributed to enhanced light absorption, increased mobility, and improved phase separation in the interpenetrating network of PTB7 and PCBM.[15]

The significant effect of the polymer molecular weight on the performance of bulk heterojunction solar cells has also been demonstrated for other polymers.[16−27] In some cases, higher molecular weight would result in improved power conversion efficiency,[17,18,22,23,26] while in others an intermediate M_w or a mixture of different molecular weights were found to result in an optimal performance.[16,19,20,24,25] Molar mass distribution was also reported to affect the solar cell performance.[27] Increased light absorption and increased charge mobility are commonly observed with increasing molecular weight of the polymer.[17,18] However, absorption is often examined by the measurement of the absorption spectra, sometimes normalized by the film thickness.[17,18,20] This does not provide sufficient information on the changes of the optical properties of the polymer. Here we performed a comprehensive spectroscopic ellipsometry (SE)[28,29] study of the PTB7:$PC_{71}BM$ thin films for different values of M_w

Received: December 2, 2014
Accepted: June 3, 2015
Published: June 3, 2015

DOI: 10.1021/am5085034
ACS Appl. Mater. Interfaces 2015, 7, 13198−13207

Table 1. Properties and Device Performance Parameters Obtained for PTB7 Material from Different Suppliers Spin Coated at 2000 rpm[a]

sample	MW (g/mol), PDI (ref)	MW (g/mol), PDI (m)	D_{rms} (nm)	S (at%)	F (at%)	d (nm)	J_{sc} (mA/cm^2)	V_{oc} (V)	FF	η (%)	μ_h (10^{-4} cm^2/(Vs))	μ_e (10^{-4} cm^2/(Vs))
A	97k, 2.3	299k, 3.0	1.4	5.1	1.5	77	15.1 ± 0.2 (15.1)	0.73 ± 0.01	0.70 ± 0.01	7.8 ± 0.1	5.90	3.74
AN	108k,2.4	335k, 3.2	1.2	4.6	1.2	88	14.7 ± 0.1 (14.5)	0.73 ± 0.01	0.71 ± 0.01	7.6 ± 0.1	4.75	3.04
B	78k, 3.6	78k, 2.2	4.0	5.9	1.5	62	11.0 ± 0.2 (10.8)	0.69 ± 0.01	0.56 ± 0.01	4.3 ± 0.1	1.33	3.86
BN	79k, 3.6	104k, 3.1	2.9	5.4	1.5	63	11.4 ± 0.2 (11.4)	0.73 ± 0.01	0.65 ± 0.01	5.4 ± 0.2	1.93	2.95
C	25k, 2.0	25k, 2.0	1.1	5.1	1.5	90	15.1 ± 0.1 (15.2)	0.74 ± 0.01	0.64 ± 0.01	7.1 ± 0.1	3.66	3.80
CN	82k, 1.6	82k, 1.6	2.0	4.9	1.2	65	14.7 ± 0.4 (14.6)	0.71 ± 0.01	0.66 ± 0.01	6.9 ± 0.2	2.49	3.74
A2	25k, 2.0	53k, 2.5	4.4	5.5	1.5	53	11.8 ± 0.4 (11.9)	0.71 ± 0.01	0.55 ± 0.01	4.6 ± 0.1	0.21	0.52
A3	50k, 2.4	70k, 2.3	3.9	5.4	1.3	53	12.5 ± 0.3 (12.6)	0.73 ± 0.01	0.60 ± 0.01	5.5 ± 0.1	0.51	0.59
A4	100k, 4.0	210k, 2.7	1.4	4.4	1.3	62	15.3 ± 0.3 (15.5)	0.72 ± 0.01	0.65 ± 0.01	7.1 ± 0.1	0.79	1.18

[a] D_{rms} denotes roughness determined using AFM. The average values and errors of performance parameters were obtained from 3 to 6 devices. J_{sc} estimated from EQE are given in brackets. Thicknesses d were obtained from ellipsometry measurement. These thickness values were used for the calculation of mobility values. For MW and PDI, (ref) denotes values provided by the manufacturer, (m) denotes measured values.

and PDI of PTB7. We examined commercially available PTB7 samples from three different suppliers, two different lot numbers for two suppliers and five different lot numbers from one supplier (1-Material). This supplier is a commonly reported supplier in the literature,[1,2,5−8,11,12] although M_w and PDI are often not listed.[1,2,5−8,11,12] In addition, the blend films were characterized by atomic force microscopy and X-ray photoelectron spectroscopy. It is well-known that the power conversion efficiency is strongly related to nanoscale morphology or microphase separation.[12,23,24] The efficiency of solar cells is also dependent on the vertical segregation and the amount of fullerene coverage at the cathode, since this affects the cathode selectivity.[5] Increased fullerene coverage at the cathode interface results in higher efficiency.[5] This is because higher presence of fullerene at the cathode interface results in lower leakage current, that is, lower undesired collection of holes at the cathode.[5] Higher leakage currents correspond to lower shunt resistances and consequently lower fill factors.[5] When fullerene coverage increased from 35% to 81%, the efficiency increased from 3.1% to 5.4%.[5] Finally, charge transport is a critical factor affecting the efficiency. The carrier mobilities were investigated using space charge limited current (SCLC) measurements.[22,30] The effects of the polymer properties on photovoltaic performance are discussed in detail. Spectroscopic ellipsometry characterization has provided insight into the effect of the polymer properties on its extinction coefficient and consequently optical absorption. However, the extinction coefficient did not appear to be the dominant factor affecting the efficiency of the devices. The efficiency appeared to be closely related to the hole mobilities, which are likely affected by the bulk heterojunction morphology. The relationship between the solar cell efficiency and the polymer properties appears to be complex. In addition, there is a significant difference in the performances of PTB7 samples from different suppliers. Possible polymer preparation and purification method likely affects the performance in addition to the molecular weight and PDI.

2. EXPERIMENTAL METHODS

PTB7 samples were obtained from 3 different suppliers: (A) 1-Material Inc. (Product number OS0007; lot number YY5220; MW = 97 000 g/mol; PDI = 2.3); (AN) 1-Material Inc. (Product number OS0007; lot number YY6116; MW = 108 000 g/mol; PDI = 2.4); (A2) 1-Material Inc. (Product number OS0007; lot number SX7111C; MW =25 000 g/mol; PDI = 2.0); (A3) 1-Material Inc. (Product number OS0007; lot number YY5215; MW =50 000 g/mol; PDI = 2.4); (A4) 1-Material Inc. (Product number OS0007; lot number SX7099; MW =100 000 g/mol; PDI = 4.0); (B) Luminescence Technology Corp. (Product number LT-S9050; lot number 130506001; MW = 78 000 g/mol; PDI = 3.6); (BN) Luminescence Technology Corp. (Product number LT-S9050; lot number 1411226002; MW = 79 000 g/mol; PDI = 3.6); (C) Organtec Materials Inc. (Product code OT-PTB7; lot number 2013041702; MW = 25 000 g/mol; PDI = 2.0); (CN) Organtec Materials Inc. (Product code OT-PTB7; lot number 20141230; MW = 82 000 g/mol; PDI = 1.6). $PC_{71}BM$ was purchased from American Dye Source, Inc. (lot number 11K005E, purity > 99.0%) or from Luminescence Technology Corp. (Product number LT-S923; lot number 201410140, purity > 99.0%). The properties and performance of blend films with PCBM from two different sources were comparable, and the source of PCBM did not have a significant effect on the obtained PCE. The molecular weight and PDI of the polymers

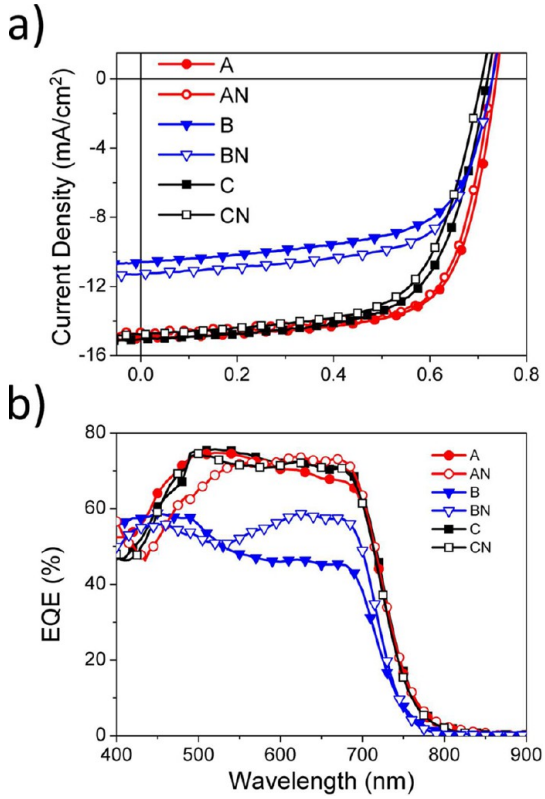

Figure 1. (a) I−V and (b) EQE curves of solar cells prepared with A,B,C-PTB7:PCBM and AN,BN,CN-PCBM with spin coating speed 2000 rpm.

DOI: 10.1021/am5085034
ACS Appl. Mater. Interfaces 2015, 7, 13198−13207

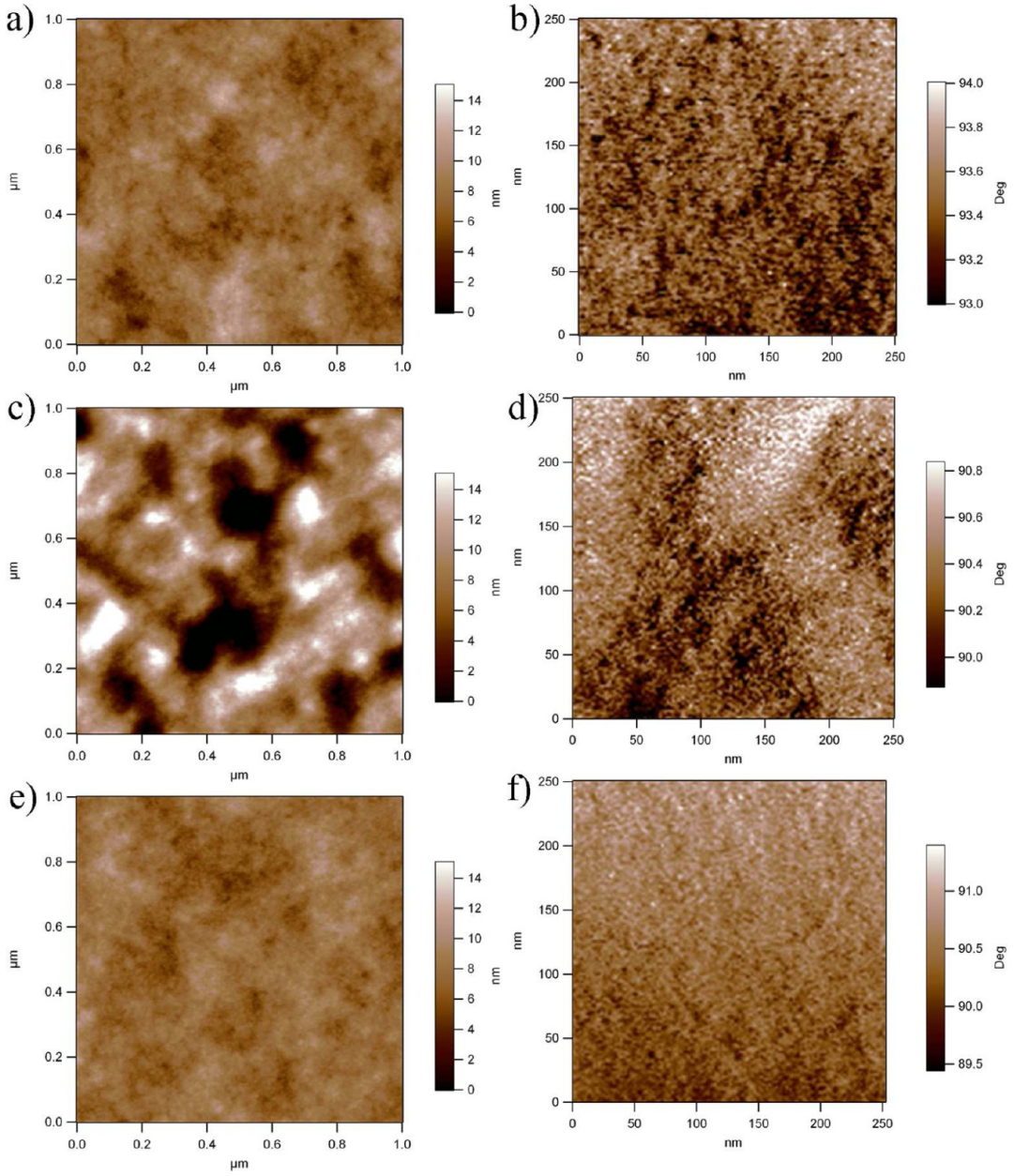

Figure 2. Topography (left) and phase (right) AFM images for (a, b) A-PTB7:PCBM, (c, d) B-PTB7:PCBM, and (e, f) C-PTB7:PCBM.

were provided by Organtec Materials Inc. company. The measurements were performed using a GPC system equipped with two Mixed-D GPC columns and RI detector. Chloroform was used as the eluent (flow rate = 1.0 mL/min) and polystyrene narrow standards were used for calibration.

Blend solutions for all the samples were prepared with the same procedures. A concentration of 25 mg/mL PTB7:$PC_{71}BM$ solution (1:1.5) was prepared by dissolving 10 mg of PTB7 and 15 mg of $PC_{71}BM$ in chlorobenzene/1,8-diiodoctane (97:3 vol %) mixed solvent. The PTB7 and $PC_{71}BM$ solutions were first stirred separately for 18 h at 45 °C and then stirred together for further 30 h. The blend solution was heated up to 70 °C for 1 h before use.

For device fabrication, the device structure was indium tin oxide (ITO)/poly(3,4-ethylene-dioxythiophene):poly(styrenesulfonate) (PEDOT:PSS)/PTB7:$PC_{71}BM$/Ca (20 nm)/Al (100 nm). The PEDOT:PSS solution (Clevios PVP Al4083) was passed through a 0.45 μm filter and spin-coated on cleaned substrates at 4000 rpm for 1 min followed by annealing at 130 °C for 20 min on a hot plate. The thickness of PEDOT:PSS film was determined to be 39 ± 4 nm. The blend solution was then spin-coated on the PEDOT:PSS at 1000, 1500, 2000, 2500, and 3000 rpm for 1 min. After drying in the glovebox overnight, methanol was spin-coated on top of the active layer at 2500 rpm for 40 s.[7] The prepared samples were then put into a thermal evaporator for electrode deposition at ~10^{-8} Torr. The device area was 0.12 cm^2. The samples were encapsulated in the glovebox before taking out for characterization. The $I-V$ characteristics of devices were measured with a Keithley 2400 sourcemeter under AM 1.5 simulated sunlight illumination (ABET Technologies SUN 2000) at 100 mW/cm^2 determined by Molectron Power Max 500D laser power meter. External quantum efficiency (EQE) was determined by a QE system from Enli Technology Co., Ltd.

For the determination of refractive index (n, k), blend solutions were spin-coated on 3 mm thick glass substrates (sufficient thickness to eliminate errors due to backside reflection in SE which is reflected outside the detector area). Each set was comprised of samples prepared at 5 different spinning speeds (1000, 1500, 2000, 2500, and 3000 rpm) to obtain different thicknesses. SE at 5 angles of incidence (55°, 60°, 65°, 70°, 75°) and transmission measurement (T) were carried out with ellipsometer M-2000DI from J.A. Woollam Inc. The multisample fitting[28,29] was carried out for the obtained

DOI: 10.1021/am5085034
ACS Appl. Mater. Interfaces 2015, 7, 13198−13207

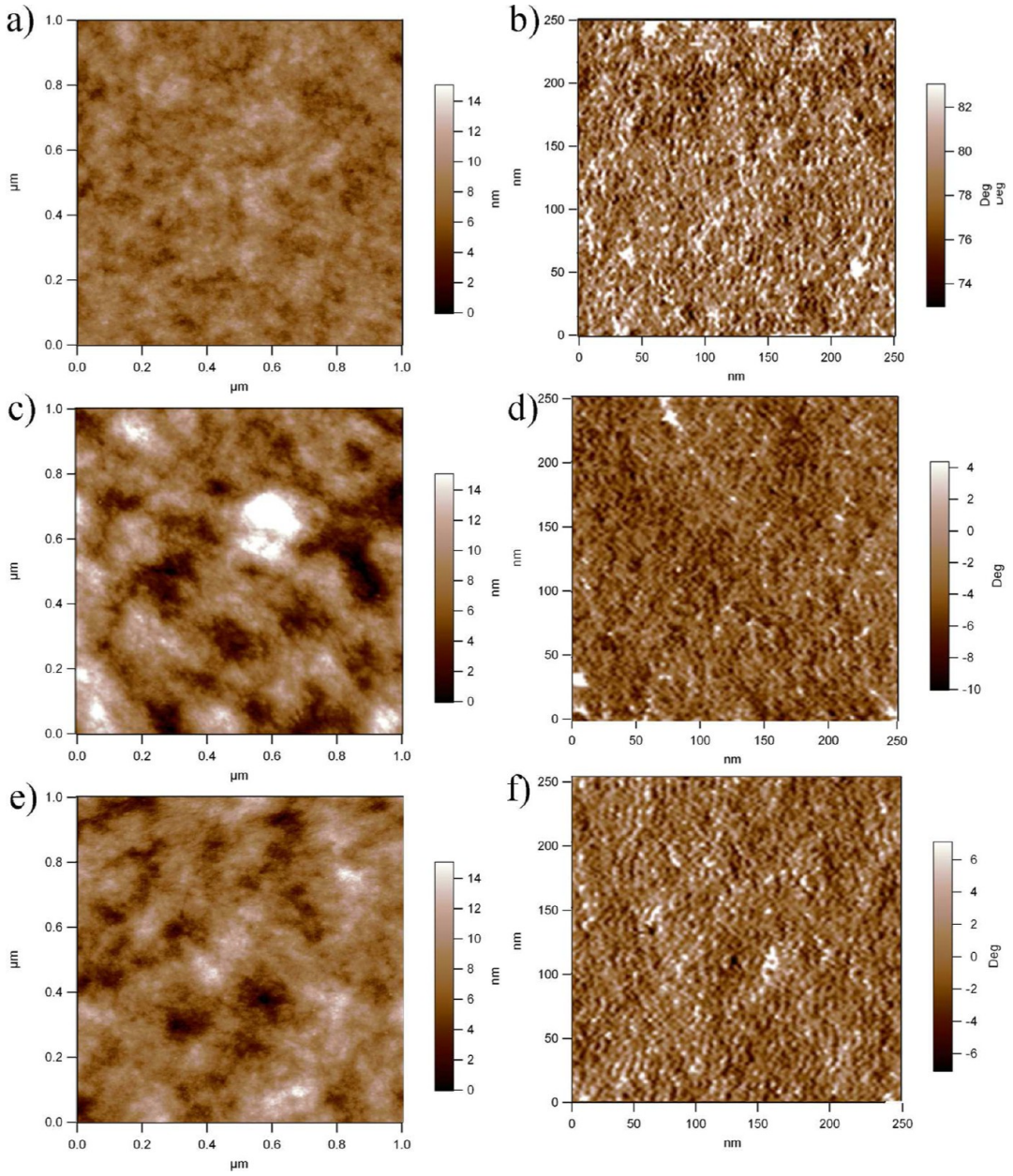

Figure 3. Topography (left) and phase (right) AFM images for (a, b) AN-PTB7:PCBM, (c, d) BN-PTB7:PCBM, and (e, f) CN-PTB7:PCBM.

values of Ψ, Δ, and T from 400 to 900 nm using WVASE32 from J.A. Woollam Inc.

The surface morphologies of the samples were characterized by Atomic Force Microscopy (AFM) using an Asylum Research MFP3D in semicontact (tapping) mode. Specific samples, prepared by spin coating at 2000 rpm on ITO substrate, were used for the determination of atomic % of sulfur and fluorine on surface of the blend films using XPS measurements performed with a Physical Electronics Quantum 2000 XPS system.

The charge carrier mobility was measured with an SCLC technique.[22,30] The device configurations were ITO/PEDOT:PSS/PTB7:$PC_{71}BM$/Au (50 nm) for hole-only devices, and ITO/Al (50 nm)/PTB7:$PC_{71}BM$/Ca (20 nm)/Al (100 nm) for electron-only devices. For hole-only devices, high work function electrodes were used for hole collection and electron blocking, while for electron-only devices low work function electrodes were used for electron collection and hole blocking. Device configurations with hole-selective and electron-selective configurations were then used for the transport measurements for holes and electrons, respectively. The PTB7:$PC_{71}BM$ blend film was prepared in the exactly the same way as in solar cell preparation. The carrier mobilities were determined using a space charge limited current equation.[22,30]

3. RESULTS AND DISCUSSION

We have investigated solar cells prepared with PTB7 from three different commercial suppliers. The properties of the polymers investigated and their photovoltaic performance parameters are summarized in Table 1, while the corresponding $I-V$ curves and EQE are shown in Figure 1 and Figure S1 (Supporting Information). It can be observed that the obtained efficiencies vary on average from 4.6% to 7.8%. The performance of three polymer samples was compared for the same device preparation conditions (the same spinning speed for spin-coating), chosen to be close to the optimal value for most of the samples, that is, 2000 rpm (the photovoltaic performance for different spinning speeds for each polymer is given in Supporting Information, the best performance is obtained for 2000 rpm for A-, AN-, A2-, A4-, BN-, C-, and CN-PTB7, while 1500 rpm results in the best

DOI: 10.1021/am5085034
ACS Appl. Mater. Interfaces 2015, 7, 13198−13207

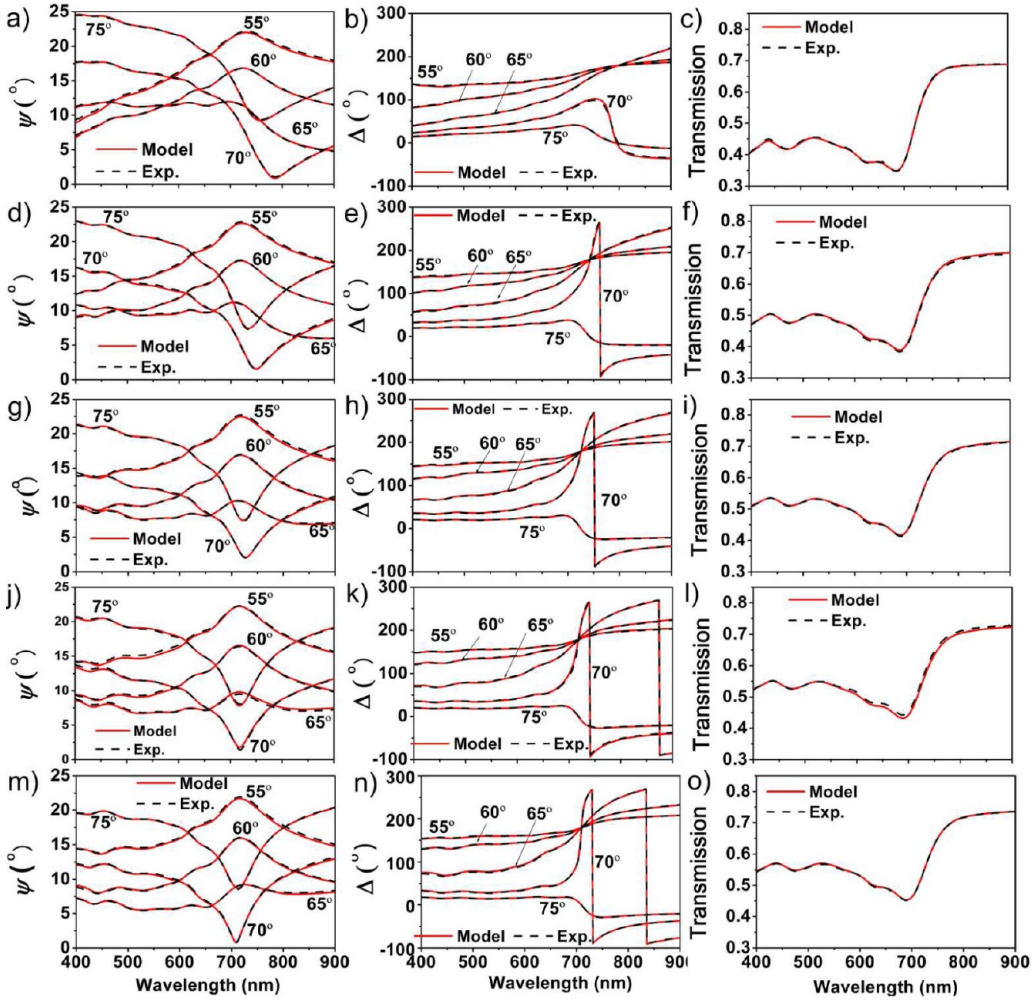

Figure 4. Model and experimental data (ellipsometry and transmission) of A-PTB7:PCBM: (a, b, c) 1000, (d, e, f) 1500, (g, h, i) 2000, (j, k, l) 2500, (m, n, o) 3000 rpm using an oscillator anisotropic model and coupled thickness for SE and *T*.

performance for B-PTB7, and 1000 rpm results in the best performance for A3-PTB7). It can be observed that the film thickness varies for different samples, despite the fact that the same spin-coating conditions were used. This is likely due to the variation in solution viscosity for different molecular weights and PDI. Nevertheless, it is obvious that there are significant performance differences for the devices with similar thickness of the active layer prepared using different PTB7 samples (Supporting Information, Tables S1−S9 for solar cell performance, Tables S19 and S20 for the thickness values.)

The charge transport and photovoltaic performance can be significantly affected by the bulk heterojunction morphology. To examine the morphology and phase separation, AFM measurements were performed, while XPS was performed to obtain information about the amount of polymer present at the top surface (cathode interface). The topography and phase contrast AFM images are shown in Figure 2, Figure 3 and Figure S2 (Supporting Information). It can be observed that the samples prepared with B-PTB7 and BN-PTB7 exhibit larger roughness and larger domain size compared to the other samples. Similar observation applies to A2-PTB7 and A3-PTB7 samples. On the other hand, the bulk heterojunction morphology for samples exhibiting high efficiency does not involve large domains or high surface roughness despite the fact that polymer samples have significantly different molecular weight (A, AN, C, CN). Unlike P3HT, PTB7 does not crystallize and the films typically show a mixture of PTB7-rich and $PC_{71}BM$-rich phases,[12] with more finely dispersed mixtures resulting in improved photovoltaic performance.[12,13] The films exhibiting differences in phase separation did not exhibit any significant differences in polymer order and orientation.[12] However, hierarchical nanomorphologies were reported for PTB7:PCBM blend films, although in this case the obtained power conversion efficiency were below 4.5%.[14] Therefore, it is not surprising that the bulk heterojunctions exhibiting poor performance has significantly different morphology (coarser phase separation) compared to the other samples which result in higher efficiency. The inferior surface morphology was reported to be correlated with reduced charge mobility in P3HT samples.[16] Furthermore, XPS data in low efficiency samples confirm that larger percentages of sulfur and fluorine can be found at the surface (see Table 1). Since sulfur and fluorine are present only in PTB7 and not in $PC_{71}BM$, increased amount of sulfur and fluorine on the surface indicates that a higher percentage of PTB7 is present at the metal electrode interface. Higher percentage of PTB7 implies lower fullerene coverage at the cathode interface, which would be unfavorable for charge collection due to increased leakage currents caused by undesired hole collection at the cathode interface.[5]

To examine the optical properties of the films prepared using the three different PTB7 samples, spectroscopic ellipsometry

DOI: 10.1021/am5085034
ACS Appl. Mater. Interfaces 2015, 7, 13198−13207

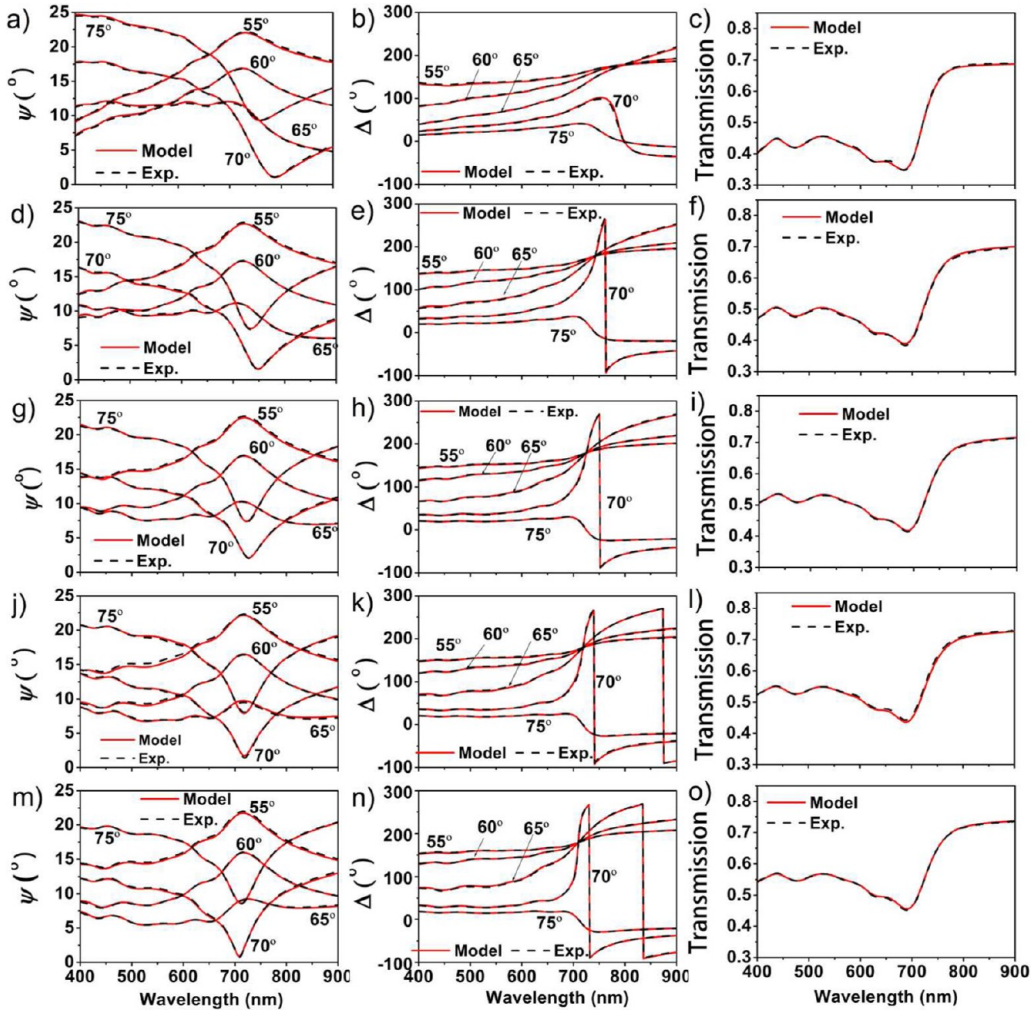

Figure 5. Model and experimental data (ellipsometry and transmission) of A-PTB7:PCBM using EMA approach using the 1000 and 3000 rpm as basis components (see text and detailed data analysis in Supporting Information) and coupled thickness for SE and *T*: (a, b, c) 1000, (d, e, f) 1500, (g, h, i) 2000, (j, k, l) 2500, and (m, n, o) 3000 rpm.

measurements were performed on films of five different thickness obtained by varying the spin coating speed. The obtained fitting results (comparison between experimental data and model calculation) for all thickness values and the model parameters are summarized in the Supporting Information. As it is standard in SE, or SE + T, data analysis,[28] we use the mean squared error (MSE) to quantify the "goodness of fit" that is the ability for an optical model to best describe the experimental data, which is also summarized in the Supporting Information.

We find that, unlike P3HT which can be described with an isotropic model without annealing,[28,29] PTB7 requires an anisotropic optical model similar to annealed P3HT.[28] Although PTB7 does not crystallize and the PTB7:$PC_{71}BM$ films typically consist of a mixture of PTB7-rich and $PC_{71}BM$-rich phases,[12] which would result in reduced likelihood of preferential ordering of polymer chains, we have verified by multiple approaches that the consideration of anisotropy was essential to obtain a simultaneous good fit to the ellipsometry and transmission values with reasonable thickness values. Different from P3HT,[28] some of the samples (certain values of thickness) exhibited a different quality of fit when all five thicknesses were considered. Thickness-dependent degree of anisotropy and polymer chain organization was previously observed in a low band gap polymer;[24] It is therefore expected that the degree of orientation of polymer chains can be affected by the film thickness (more oriented in thin films, less oriented in thick films). To improve the quality of the fit, we have considered the case where the optical properties for the films with intermediate thickness values result from a homogeneous mixture, which can be modeled using an effective medium approximation of the optical properties obtained from separately fits for the thinnest (3000 rpm) and the thickest (1000 rpm) films (see Supporting Information for fitting parameters). The fit quality is improved, without significantly increasing the complexity of the model used. The comparison between the EMA fitting and the simultaneous 5 thickness fitting for A-PTB7:PCBM is shown in Figures 4 and 5, respectively (see Supporting Information for remaining samples, since the differences in the fit quality between two fitting approaches are similar). The differences in the obtained index of refraction between the two approaches are small, and mainly in the obtained index of refraction values for the parallel polarization and they are the most pronounced for samples B and BN.

The obtained values of the real and imaginary parts of the index of refraction, *n* and *k*, for two polarizations are shown in Figure 6. We can observe that for perpendicular polarization, which has larger influence on the measured optical properties, the extinction coefficients of samples A2, A3, B and BN in the

DOI: 10.1021/am5085034
ACS Appl. Mater. Interfaces 2015, 7, 13198−13207

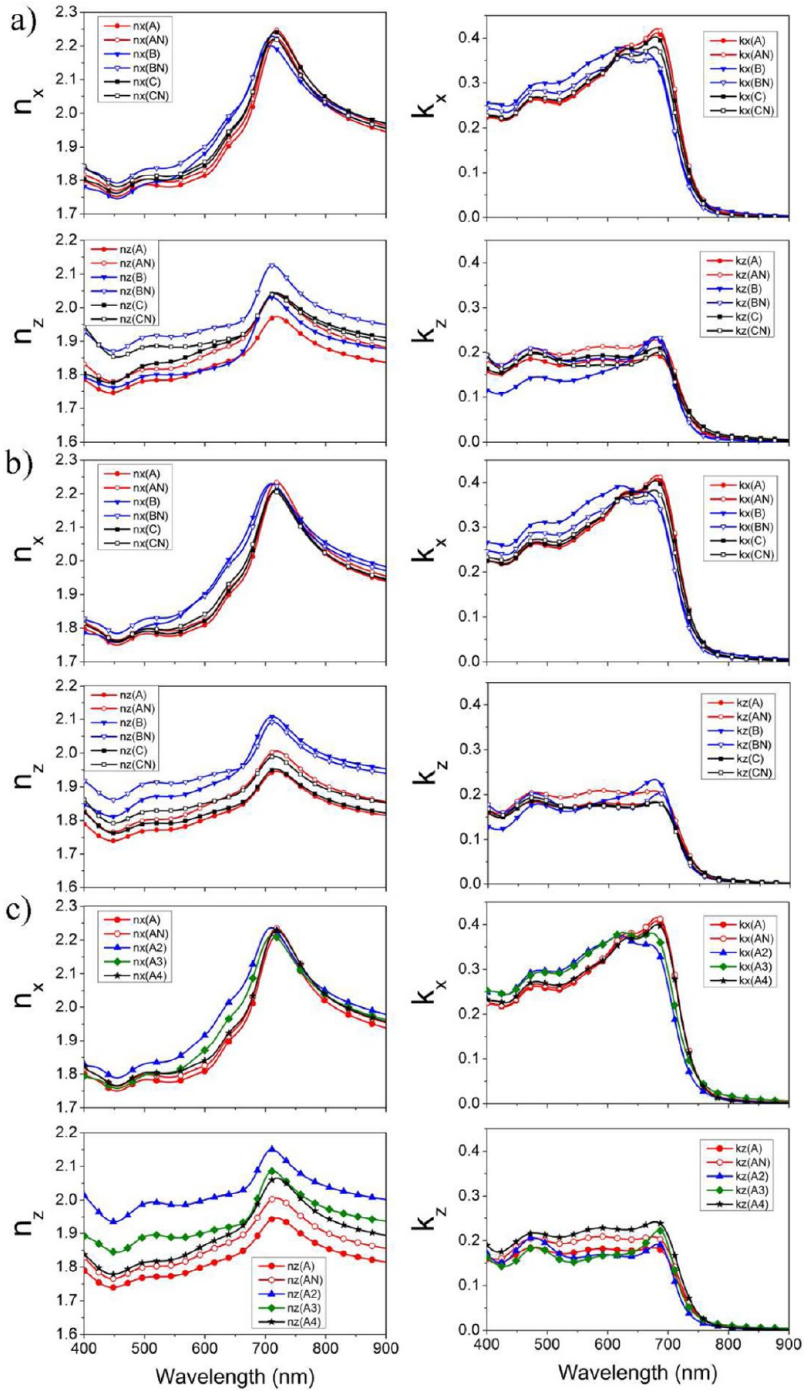

Figure 6. Ordinary and extraordinary real (n_x, n_z) and imaginary (k_x, k_z) values of the refractive index of A, AN, B, BN, C, and CN-PTB7:PCBM blends obtained by (a) using an oscillator anisotropic model and coupled thickness for SE and *T* and fitting all five thicknesses simultaneously. (b) EMA approximation for the 2000 rpm film using optical properties of 1000 and 3000 rpm films as basis components. (c) Refractive index of A, AN, A2, A3, and A4-PTB7:PCBM blends obtained by EMA approximation for the 2000 rpm film using optical properties of 1000 and 3000 rpm films as basis components.

region below 600 nm are smaller than those of A, AN, C, and CN. However, the lowest energy transition (peak in k_x at ~680 nm) is more pronounced in the samples A, AN, A4, C, and CN. Nevertheless, the small differences in the extinction coefficients are not expected to result in significant enough differences in the absorption of the cells and thus cannot explain the difference in photovoltaic performance. The overall absorption is smaller for samples B and BN because of their lower thickness, but there is no clear relationship between the calculated absorption of the film (k_xD/λ, where *D* is the film thickness for 2000 rpm spinning speed) and the power conversion efficiency for different PTB7 samples.

Photovoltaic performance is affected by both optical absorption and charge transport. To examine charge transport in more detail, the electron and hole mobilities were determined from SCLC measurements,[22,30] as shown in Figure 7. It can be observed that the mobility trends follow the trend of PCE, indicating that the charge transport significantly affects the efficiency.

DOI: 10.1021/am5085034
ACS Appl. Mater. Interfaces 2015, 7, 13198−13207

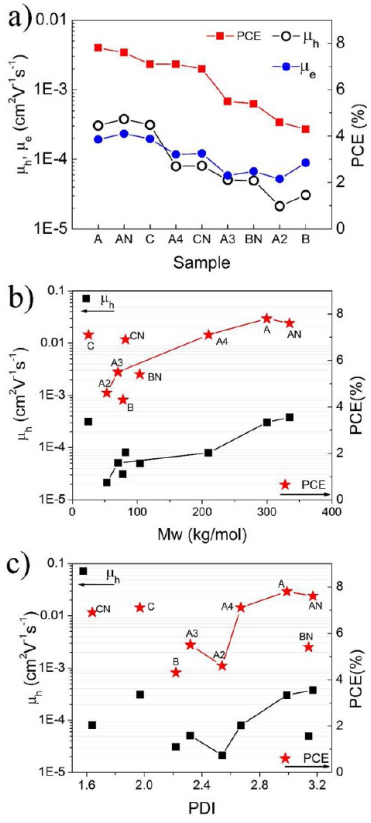

Figure 7. Electron (μ_e) and hole (μ_h) mobilities of different samples; dependence of hole mobilities (b) on molecular weight and (c) on polydispersity. MW and PDI are measured values. PCE values are also shown for comparison.

The obtained values for the electron mobility are somewhat lower compared to a previous report (2.1×10^{-3} cm^2 $V^{-1}s^{-1}$).[7] The hole mobilities obtained are comparable to the previous reports (1.6×10^{-4} cm^2 $V^{-1}s^{-1}$ and $2.85-6.30 \times 10^{-4}$ cm^2 $V^{-1}s^{-1}$).[7,15] However, unlike previous work which found that hole mobility increases with increased molecular weight,[15] no such clear molecular weight dependence can be observed in our work when comparing the PTB7 provided from three different suppliers. It is possible that the optimized PTB7 synthesis procedures and conditions would not be the same among the suppliers, which will affect the trends of hole mobility of the samples. This is also likely because charge transport is also related to PDI, with smaller PDI (samples C and CN compared to samples B and BN) likely to result in more regularly ordered molecular structure which is more favorable for charge transfer.[15] It was previously shown that the decreasing hole mobility with decreasing molecular weight can be attributed to the increased charge hopping distances because of less efficient intermolecular charge transfer.[22] However, the effect of PDI was not investigated.[22] Nevertheless, it can be expected that both MW and PDI would affect the availability of the hopping sites and thus the probability of intermolecular charge transfer and consequently the charge mobility.[22]

To study the effect of molecular weight on carrier mobility more comprehensively and exclude the influence of different synthesis methods, we further conducted the experiments by using the PTB7 with different molecular weight synthesized by the same supplier. If we consider only the data from the same supplier (A, AN, A2, A3, A4) we can see that there is an increase in hole mobility and power conversion efficiency with increasing molecular weight. The dependence on PDI is less clear. Comparing different suppliers, high efficiency can be achieved for both large MW and large PDI (A, AN, A4) or lower MW and low PDI (C, CN). However, due to large differences in the performance of the samples with similar properties in terms of MW and PDI (B, A3), as well as large variation of performance among different suppliers for samples with lower molecular weights, we can also conclude that the polymer synthesis and purification process may have a significant influence on the photovoltaic performance. Contrary to a recent study which examined 5 commercial samples (four from Solarischem and one from Solarmer),[27] the samples that exhibited low efficiency (B, BN, A2, A3, see Supporting Information) do not show bimodal distribution in the molecular weight distribution curves. Thus, it is clear that presence of substantial amount of low molecular weight components[27] is not the only factor which can result in an unfavorable bulk heterojunction morphology. We clearly demonstrated that efficient solar cells can be achieved both for large M_w and large PDI (A, AN, A4) or lower MW and low PDI (C, CN). The difference between our results and the report on the effect of polymer distribution is likely because of different commercial sources of polymer, and possibly different experimental conditions for gel permeation chromatography (GPC) measurements. However, it should be noted that we used more samples from one supplier as well as more suppliers compared to other reports.[15,27] From the fact that all 3 low performance samples came from the same supplier,[27] it can be concluded that other factors such as polymer synthesis and purification are equally important as the presence of low molecular weight species that contributed to the inferior photovoltaic performance. It should be noted, however, that in our study as well we found that samples exhibiting coarser morphology (B, BN, A2, A3) exhibit lower power conversion efficiency. The dependence of the film morphology and phase separation on the PTB7 properties is likely complex, and it is possible to obtain favorable morphology and high efficiency with more than one combination of polymer properties in terms of MW, PDI, and the molecular weight distribution.

It should also be pointed out that, as expected, there is a small variation in the performance between samples with different lot numbers for the same commercial suppliers. For each supplier, the performance between the lot numbers with similar polymer properties is reasonably consistent, with B and BN exhibiting the largest difference in performance and properties. For these particular samples, the polymer powder also appears to be different upon observation by a naked eye (loose powder vs large clumps). This can possibly occur due to broad distribution of the molecular weights in B and BN samples, and possibly related to polymer synthesis and purification process used since other samples with large PDI can exhibit high efficiency.

4. CONCLUSION

We have studied the properties and photovoltaic performance of PTB7:$PC_{71}BM$ blend films, for different molecular weights and polydispersity indices of PTB7. We have performed a comprehensive morphological, optical and electronic characterization of the films. We found that PTB7 properties affected the bulk heterojunction morphology, extinction coefficient and charge transport. The cells with the lower efficiency exhibited coarse phase separation with large domain size and higher surface roughness, lower extinction coefficient for the lowest energy transition for perpendicular polarization, and lower hole

DOI: 10.1021/am5085034
ACS Appl. Mater. Interfaces 2015, 7, 13198−13207

mobilities. These samples generally exhibited larger PDI values in combination with lower Mw. Good photovoltaic performance (PCE 6.9−7.8%) could be obtained with a wide range of PTB7 properties (higher MW with higher PDI, or lower MW with lower PDI).

■ ASSOCIATED CONTENT

Supporting Information

Solar cell performance (J_{sc}, V_{oc}, η), fitting results and parameters of SE and T for different fitting options using A, AN, A2, A3, A4, B, BN, C, and CN-PTB7:PCBM; ellipsometry fitting results for AN, A2, A3, A4, BN, and CN-PTB7:PCBM; AFM images for A2, A3, and A4-PTB7:PCBM; comparison of the obtained index of refraction for various PTB7:PCBM for different fitting options; XPS data; and molecular mass distributions of different samples. The Supporting Information is available free of charge on the ACS Publications website at DOI: 10.1021/am5085034.

■ AUTHOR INFORMATION

Corresponding Authors

*Tel: +852 2859 7946. Fax: +852 2559 9152. E-mail: dalek@hku.hk.

*Tel: +852 3442 7823. Fax: +852 3442 0541. E-mail: apjazs@cityu.edu.hk.

Notes

The authors declare no competing financial interest.

■ ACKNOWLEDGMENTS

This work was supported by the Strategic Research Theme, University Development Fund, and Small Project Grant (administrated by The University of Hong Kong) are also acknowledged. J.A.Z. acknowledges funding from GRF Project 122812 from the Research Grants Council of Hong Kong. Partial support of the work is provided by the RGC Theme-based Research Scheme (Grant Number HKU T23-713/11). C.S. would like to acknowledge funding support from the Clarea Au Endowment Professorship. The authors would like to thank Organtec Materials Inc. for GPC measurements.

■ REFERENCES

(1) Kohlstädt, M.; Grein, M.; Reinecke, P.; Kroyer, T.; Zimmermann, B.; Würfel, U. Inverted ITO-and PEDOT:PSS-Free Polymer Solar Cells With High Power Conversion Efficiency. *Sol. Energy Mater. Sol. Cells* **2013**, *117*, 98−102.

(2) Ochiai, S.; Imamura, S.; Kannappan, S.; Palanisamy, K.; Shin, P.-K. Characteristics and the Effect of Additives on the Nanomorphology of PTB7/$PC_{71}BM$ Composite Films. *Curr. Appl. Phys.* **2013**, *13*, S58−S63.

(3) Yonezawa, K.; Kamioka, H.; Yasuda, T.; Han, L.; Moritomo, Y. Exciton-to-Carrier Conversion Processes in a Low-Band-Gap Organic Photovoltaic. *Jpn. J. Appl. Phys.* **2013**, *S2*, No. 062405.

(4) Zhang, W.; Zhao, B.; He, Z.; Zhao, X.; Wang, H.; Yang, S.; Wu, H.; Cao, Y. High-Efficiency ITO-Free Polymer Solar Cells Using Highly Conductive PEDOT:PSS/Surfactant Bilayer Transparent Anodes. *Energy Environ. Sci.* **2013**, *6*, 1956−1964.

(5) Guerrero, A.; Dörling, B.; Ripolles-Sanchis, T.; Aghamohammadi, M.; Barrena, E.; Campoy-Quiles, M.; Garcia-Belmonte, G. Interplay Between Fullerene Surface Coverage and Contact Selectivity of Cathode Interfaces in Organic Solar Cells. *ACS Nano* **2013**, *7*, 4637−4646.

(6) Chang, Y.-M.; Su, Y.-Y.; Leu, C.-Y. Improvement in Power Conversion Efficiency of Organic Photovoltaic Devices by Using Excimer Ultraviolet-Radiation Induced Mesoporous Silica Anti-Reflection Coating. *Thin Solid Films* **2013**, *534*, 492−496.

(7) Zhou, H.; Zhang, Y.; Seifter, J.; Collins, S. D.; Luo, C.; Bazan, G. C.; Nguyen, T. Q.; Heeger, A. J. High-Efficiency Polymer Solar Cells Enhanced by Solvent Treatment. *Adv. Mater.* **2013**, *25*, 1646−1652.

(8) Guerrero, A.; Montcada, N. F.; Ajuria, J.; Etxebarria, I.; Pacios, R.; Garcia-Belmonte, G.; Palomares, E. Charge Carrier Transport and Contact Selectivity Limit the Operation of PTB7-Based Organic Solar Cells of Varying Active Layer Thickness. *J. Mater. Chem. A* **2013**, *1*, 12345−12354.

(9) Lou, S. J.; Szarko, J. M.; Xu, T.; Yu, L.; Marks, T. J.; Chen, L. X. Effects of Additives on the Morphology of Solution Phase Aggregates Formed by Active Layer Components of High-Efficiency Organic Solar Cells. *J. Am. Chem. Soc.* **2011**, *133*, 20661−20663.

(10) Carsten, B.; Szarko, J. M.; Son, H. J.; Wang, W.; Lu, L.; He, F.; Rolczynski, B. S.; Lou, S. J.; Chen, L. X.; Yu, L. Examining the Effect of the Dipole Moment on Charge Separation in Donor Acceptor Polymers for Organic Photovoltaic Applications. *J. Am. Chem. Soc.* **2011**, *133*, 20468−20475.

(11) He, Z.; Zhong, C.; Huang, X.; Wong, W.-Y.; Wu, H.; Chen, L.; Su, S.; Cao, Y. Simultaneous Enhancement of Open-Circuit Voltage, Short-Circuit Current Density, and Fill Factor in Polymer Solar Cells. *Adv. Mater.* **2011**, *23*, 4636−4643.

(12) Hammond, M. R.; Kline, R. J.; Herzing, A. A.; Richter, L. J.; Germack, D. S.; Ro, H.-W.; Soles, C. L.; Fischer, D. A.; Xu, T.; Yu, L. P.; Toney, M. F.; DeLongchamp, D. M. Molecular Order in High-Efficiency Polymer/Fullerene Bulk Heterojunction Solar Cells. *ACS Nano* **2011**, *5*, 8248−8257.

(13) Liang, Y.; Xu, Z.; Xia, J.; Tsai, S. T.; Wu, Y.; Li, G.; Ray, C.; Yu, L. For the Bright Future—Bulk Heterojunction Polymer Solar Cells with Power Conversion Efficiency of 7.4%. *Adv. Mater.* **2010**, *22*, E135−E138.

(14) Chen, W.; Xu, T.; He, F.; Wang, W.; Wang, C.; Strzalka, J.; Liu, Y.; Wen, J. G.; Miller, D. J.; Chen, J. H.; Hong, K. L.; Yu, L. P.; Darling, S. B. Hierarchical Nanomorphologies Promote Exciton Dissociation in Polymer/Fullerene Bulk Heterojunction Solar Cells. *Nano Lett.* **2011**, *11*, 3707−3713.

(15) Liu, C.; Wang, K.; Hu, X.; Yang, Y.; Hsu, C.-H.; Zhang, W.; Xiao, S.; Gong, X.; Cao, Y. Molecular Weight Effect on the Efficiency of Polymer Solar Cells. *ACS Appl. Mater. Interfaces* **2013**, *5*, 12163−12167.

(16) Ballantyne, A. M.; Chen, L.; Dane, J.; Hammant, T.; Braun, F. M.; Heeney, M.; Duffy, W.; McCulloch, I.; Bradley, D. D. C.; Nelson, J. The Effect of Poly(3-Hexylthiophene) Molecular Weight on Charge Transport and the Performance of Polymer:Fullerene Solar Cells. *Adv. Funct. Mater.* **2008**, *18*, 2373−2380.

(17) Chu, T.-Y.; Lu, J.; Beaupré, S.; Zhang, Y.; Pouliot, J.-R.; Zhou, J.; Najari, A.; Leclerc, M.; Tao, Y. Effects of the Molecular Weight and the Side-Chain Length on the Photovoltaic Performance of Dithienosilole/Thienopyrrolodione Copolymers. *Adv. Funct. Mater.* **2012**, *22*, 2345−2351.

(18) Osaka, I.; Saito, M.; Mori, H.; Koganezawa, T.; Takimiya, K. Drastic Change of Molecular Orientation in a Thiazolothiazole Copolymer by Molecular-Weight Control and Blending with $PC_{61}BM$ Leads to High Efficiencies in Solar Cells. *Adv. Mater.* **2012**, *24*, 425−430.

(19) Ma, W.; Kim, J. Y.; Lee, K.; Heeger, A. J. Effect of the Molecular Weight of Poly(3-Hexylthiophene) on the Morphology and Performance of Polymer Bulk Heterojunction Solar Cells. *Macromol. Rapid Commun.* **2007**, *28*, 1776−1780.

(20) Hiorns, R. C.; de Bettignies, R.; Leroy, J.; Bailly, S.; Firon, M.; Sentein, C.; Khoukh, A.; Preud'homme, H.; Dagron-Lartigau, C. High Molecular Weights, Polydispersities, and Annealing Temperatures in the Optimization of Bulk-Heterojunction Photovoltaic Cells Based on Poly(3-Hexylthiophene) or Poly(3-Butylthiophene). *Adv. Funct. Mater.* **2006**, *16*, 2263−2273.

(21) Schilinsky, P.; Asawapirom, U.; Scherf, U.; Biele, M.; Brabec, C. J. Influence of the Molecular Weight of Poly(3-Hexylthiophene) on

DOI: 10.1021/am5085034
ACS Appl. Mater. Interfaces 2015, 7, 13198−13207

the Performance of Bulk Heterojunction Solar Cells. *Chem. Mater.* **2005**, *17*, 2175−2180.
(22) Lee, H. K. H.; Li, Z.; Constantinou, I.; So, F.; Tsang, S. W.; So, S. K. Bath-to-Batch Variation of Polymeric Photovoltaic Materials: Its Origin and Impacts on Charge Carrier Transport and Device Performances. *Adv. Energy Mater.* **2014**, *4*, 1400768.
(23) Bartelt, J. A.; Douglas, J. D.; Mateker, W. R.; El Labban, A.; Tassone, C. J.; Toney, M. F.; Fréchet, J. M. J.; Beaujuge, P. M.; McGeehee, M. D. Controlling Solution-phase Polymer Aggregation with Molecular Weight and Solvent Additives to Optimize Polymer-Fullerene Bulk Heterojunction Solar Cells. *Adv. Energy Mater.* **2014**, *4*, No. 1301733.
(24) Liu, F.; Chen, D.; Wang, C.; Luo, K. Y.; Gu, W. Y.; Briseno, A. L.; Hsu, J. W. P.; Russel, T. P. Molecular Weight Dependence of the Morphology in P3HT:PCBM Solar Cells. *ACS Appl. Mater. Interfaces* **2014**, *6*, 19876−19887.
(25) Kim, Y. S.; Lee, Y.; Lee, W. J.; Park, H.; Han, S. H.; Lee, S. H. Effects of Molecular Weight and Polydispersity of Poly(3-hexylthiophene) in Bulk Heterojunction Polymer Solar Cells. *Curr. Appl. Phys.* **2010**, *10*, 329−332.
(26) Moet, D. J. D.; Lenes, M.; Kotlarski, J. D.; Veenstra, S. C.; Sweelssen, J.; Koetse, M. M.; de Boer, B.; Blom, P. W. M. Impact of Molecular Weight on Charge Carrier Dissociation in Solar Cells from a Polyfluorene Derivative. *Org. Electron.* **2009**, *10*, 1275−1281.
(27) Vangerven, T.; Verstappen, P.; Drijkoningen, J.; Dierckx, W.; Himmelberger, S.; Salleo, A.; Vanderzande, D.; Maes, W.; Manca, J. V. Molar Mass versus Polymer Solar Cell Performance: Highlighting the role of Homocouplings. *Chem. Mater.* **2015**, DOI: 10.1021/acs.chemmater.5b00939.
(28) Ng, A.; Li, C. H.; Fung, M. K.; Djurišić, A. B.; Zapien, J. A.; Chan, W. K.; Cheung, K. Y.; Wong, W.-Y. Accurate Determination of the Index of Refraction of Polymer Blend Films by Spectroscopic Ellipsometry. *J. Phys. Chem. C* **2010**, *114*, 15094−15101.
(29) Ng, A.; Liu, X.; To, C. H.; Djurišić, A. B.; Zapien, J. A.; Chan, W. K. Annealing of P3HT:PCBM Blend Film—The Effect on Its Optical Properties. *ACS Appl. Mater. Interfaces* **2013**, *5*, 4247−4259.
(30) Tse, S. C.; Tsang, S. W.; So, S. K. Polymeric Conducting Anode for Small Organic Transporting Molecules in Dark Injection Experiments. *J. Appl. Phys.* **2006**, *100*, No. 063708.

DOI: 10.1021/am5085034
ACS Appl. Mater. Interfaces 2015, 7, 13198−13207